The 'window' component of the low threshold Ca^{2+} current produces input signal amplification and bistability in cat and rat thalamocortical neurones

Stephen R. Williams, Tibor I. Tóth, Jonathan P. Turner, Stuart W. Hughes and Vincenzo Crunelli*

Physiology Unit, School of Molecular and Medical Biosciences, University of Wales Cardiff, Museum Avenue, Cardiff CF1 1SS, UK

1. The mechanism underlying a novel form of input signal amplification and bistability was investigated by intracellular recording in rat and cat thalamocortical (TC) neurones maintained in slices and by computer simulation with a biophysical model of these neurones.

2. In a narrow membrane potential range centred around −60 mV, TC neurones challenged with small (10–50 pA), short (50–200 ms) current steps produced a stereotyped, large amplitude hyperpolarization (> 20 mV) terminated by the burst firing of action potentials, leading to amplification of the duration and amplitude of the input signal, that is hereafter referred to as input signal amplification.

3. In the same voltage range centred around −60 mV, single evoked EPSPs and IPSPs also produced input signal amplification, indicating that this behaviour can be triggered by physiologically relevant stimuli. In addition, a novel, intrinsic, low frequency oscillation, characterized by a peculiar voltage dependence of its frequency and by the presence of plateau potentials on the falling phase of low threshold Ca^{2+} potentials, was recorded.

4. Blockade of pure Na^+ and K^+ currents by tetrodotoxin (1 μM) and Ba^{2+} (0·1–2·0 mM), respectively, did not affect input signal amplification, neither did the presence of excitatory or inhibitory amino acid receptor antagonists in the perfusion medium.

5. A decrease in $[Ca^{2+}]_o$ (from 2 to 1 mM) and an increase in $[Mg^{2+}]_o$ (from 2 to 10 mM), or the addition of Ni^{2+} (2–3 mM), abolished input signal amplification, while an increase in $[Ca^{2+}]_o$ (from 2 to 8 mM) generated this behaviour in neurones where it was absent in control conditions. These results indicate the involvement of the low threshold Ca^{2+} current (I_T) in input signal amplification, since the other Ca^{2+} currents of TC neurones are activated at potentials more positive than −40 mV.

6. Blockade of the slow inward mixed cationic current (I_h) by 4-(*N*-ethyl-*N*-phenylamino)-1,2-dimethyl-6-(methylamino)-pyrimidinium chloride (ZD 7288) (100–300 μM) did not affect the expression of the large amplitude hyperpolarization, but abolished the subsequent repolarization to the original membrane potential. In this condition, therefore, input signal amplification was replaced by bistable membrane behaviour, where two stable membrane potentials separated by 15–30 mV could be switched between by small current steps.

7. Computer simulation with a model of a TC neurone, which contained only I_T, I_h, K^+ leak current (I_{Leak}) and those currents responsible for action potentials, accurately reproduced the qualitative and quantitative properties of input signal amplification, bistability and low frequency oscillation, and indicated that these phenomena will occur at some value of the injected DC if, and only if, the 'window' component of I_T ($I_{T,Window}$) and the leak conductance (g_{Leak}) satisfy the relation $(dI_{T,Window}/dV)_{max} > g_{Leak}$.

8. The physiological implications of these findings for the electroresponsiveness of TC neurones are discussed, and, as I_T is widely expressed in the central nervous system, we suggest that 'window' I_T will markedly affect the integrative properties of many neurones.

* To whom correspondence should be addressed.

Thalamocortical (TC) neurones express a rich repertoire of voltage-activated membrane currents that produce non-linear behaviour and integration of synaptic potentials, typified, for example, by the generation of intrinsic oscillatory activity (i.e. pacemaker or delta oscillations) (McCormick & Pape, 1990; Leresche, Lightowler, Soltesz, Jassik-Gerschenfeld & Crunelli, 1991; Steriade, Curró Dossi & Nuñez, 1991; Steriade, McCormick & Sejnowski, 1993). A membrane current of particular importance to these phenomena is the low voltage activated, inactivating Ca^{2+} current (I_T) (Coulter, Huguenard & Prince, 1989; Crunelli, Lightowler & Pollard, 1989; Huguenard, 1996), whose activation underlies the generation of transient depolarizing potentials (named low threshold Ca^{2+} potentials, LTCPs) that may evoke single, or a burst of, action potentials. The amplification of the duration and amplitude of excitatory postsynaptic potentials (EPSPs) involving LTCPs has been demonstrated (Deschênes, Paradis, Roy & Steriade, 1984; Jahnsen & Llinás, 1984*a*,*b*; Crunelli, Kelly, Leresche & Pirchio, 1987*a*; Llinás, 1988; Turner, Leresche, Guyon, Soltesz & Crunelli, 1994; Bal, von Krosigk & McCormick, 1995), whilst inhibitory postsynaptic potentials (IPSPs) may lead to the generation of LTCPs crowned by the burst firing of action potentials, indicating that IPSPs may have excitatory actions (Crunelli & Leresche, 1991; Steriade *et al.* 1991, 1993). Membrane potential bistability, another type of non-linear behaviour, has been observed in TC neurones in the form of plateau potentials generated by a persistent Na^+ current (Jahnsen & Llinás, 1984*a*,*b*). No experimental evidence, however, is available in support of the formation of bistable behaviour based on the properties of I_T, as has been suggested by modelling studies (Tóth & Crunelli, 1993).

In common with other inactivating membrane currents, the steady-state activation and inactivation curves of I_T have been shown to possess a region of overlap (Coulter *et al.* 1989; Crunelli *et al.* 1989; Hernandez-Cruz & Pape, 1989; Huguenard, 1996) which may be taken as evidence for the existence of a stationary or 'window' current. The physiological expression of window currents has received little examination, although the existence of a window component of the fast Na^+ current (I_{Na}) and the fast and slowly inactivating K^+ currents (I_A and I_{AS}, respectively) has been indicated (McCormick, 1991; McCormick & Huguenard, 1992). Furthermore, no analysis of the contribution of window currents to the integration of synaptic potentials has been documented in TC or other types of central neurones. In this paper, by the use of experiments and computer simulations, we demonstrate that the window component of I_T has a dramatic influence upon the electroresponsiveness and input–output relationship of TC neurones by playing a central role in the generation of a large amplitude hyperpolarization in response to EPSPs and IPSPs, in a novel type of intrinsic low frequency oscillatory activity and in membrane potential bistability. Some of these results have been published in prelimary form (Tóth & Crunelli, 1993; Tóth, Williams, Turner & Crunelli, 1995; Williams, Turner, Tóth & Crunelli, 1995; Crunelli, Williams, Turner, Hughes & Tóth, 1997).

METHODS

Slice preparation and recording procedures

Male Wistar rats (150–200 g) were killed by decapitation according to licence. Young adult male and female cats (1–1·5 kg) were deeply anaesthetized with a mixture of O_2 and NO_2 (2:1) and 1% halothane. The top of the skull was exposed, a wide craniotomy performed and the meninges were removed. The animals were killed by a coronal cut at the level of the inferior colliculus, and, following transection of the optic tracts, the brain was removed and submerged in ice-cold (1–4 °C), oxygenated (95% O_2–5% CO_2) modified Krebs medium containing (mM): KCl, 5; KH_2PO_4, 1·25; $MgSO_4$, 5; $CaCl_2$, 1; $NaHCO_3$, 16; glucose, 10; sucrose, 250. Slices were left in the storage chamber for at least 1 h before being transferred to a recording chamber where they were perfused with a continuously oxygenated (95% O_2–5% CO_2) medium of similar composition, but with 1 mM $MgSO_4$ plus 2 mM $CaCl_2$ replacing the 5 mM $MgSO_4$ plus 1 mM $CaCl_2$, respectively. Other details of the preparation and maintenance of rat and cat slices were identical to those fully described in the accompanying paper (Turner, Anderson, Williams & Crunelli, 1997), and by Turner *et al.* (1994) and Williams, Turner, Anderson & Crunelli (1996). When $BaCl_2$ or $NiCl_2$ were ultimately to be added to the recording medium KH_2PO_4 was omitted and $MgSO_4$ was replaced with equimolar $MgCl_2$. Intracellular recordings were made from the cat ventrobasal thalamus (mainly the ventro posteriolateral and ventro posteriomedial nuclei) and the cat and rat dorsal lateral geniculate nucleus with glass microelectrodes (GC 120F; Clark Electromedical Instruments) filled with 1 M potassium acetate, or 2% (w/v) biocytin dissolved in 1 M potassium acetate. Potentials and currents were recorded using an Axoclamp-2A amplifier (Axon Instruments), configured in bridge balance, and were stored on a Biologic DAT recorder (Intracel, Royston, UK). Data were subsequently digitally sampled, and analysed using a microcomputer running pCLAMP software (Axon Instruments). In current clamp experiments, input conductance was calculated as the reciprocal of the apparent input resistance measured in the steady state. In voltage clamp experiments, input conductance (g_{in}) was calculated from the equation $g_{in} = I_S/(V - V_H)$, where I_S is steady-state current, V is command potential and V_H is holding potential. Synaptic potentials were evoked by electrical stimuli (1–10 V, 20–50 μS at 0·05 Hz) applied to a bipolar tungsten electrode placed in the optic tract or within the nucleus reticularis thalami (for TC neurones of the dorsal lateral geniculate nucleus and the ventrobasal thalamus, respectively). The following drugs were applied in the perfusion medium: 6-cyano-7-nitroquinoxaline-2,3-dione (CNQX); 1-(4-aminophenyl)-4-methyl-7,8-methylene-dioxy-5H-2,3-benzodiazepine (GYKI 52466); D,L-2-amino-5-phosphonovaleric acid (APV); (5*R*,10*S*)-(+)-5-methyl-10,11-dihydro-5H-dibenzo[*a*,*d*]-cyclohepten-5,10-imine hydrogen maleate (MK 801); *P*-(3-aminopropyl)-*P*-diethoxymethl-phosphinic acid (CGP 35348); 4-(*N*-ethyl-*N*-phenylamino)-1,2-dimethyl-6-(methylamino)-pyrimidinium chloride (ZD 7288) and bicuculline methiodide. Drugs were obtained from the following sources: CNQX and APV, Tocris-Cookson; bicuculline methiodide and tetrodotoxin, Sigma; CGP 35348, MK 801 and ZD 7288 were kindly donated by Dr W. Froestl (Novartis, Switzerland), Merk, Sharpe & Dolme (UK) and Dr P. Marshall (Zeneca, UK), respectively.

Each neurone that was successfully recovered ($n = 6$) and which showed the unusual biophysical properties described in this paper, had morphological features typical of TC neurones of the

ventrobasal thalamus (Turner *et al.* 1997) or the dorsal lateral geniculate nucleus (Crunelli, Leresche & Parnavelas, 1987*b*; Williams *et al.* 1996) (for details of biocytin injection and morphological analysis, see Williams *et al.* 1996; Turner *et al.* 1997). Analysis of the frequency of oscillatory activity was accomplished by the construction of cumulative integrative frequency plots of inter-event intervals, where each event represented the first action potential on a LTCP or the rising phase of a LTCP. This analysis was carried out for segments of data (> 1 min duration) gathered in the presence of different values of direct current (DC) injected through the recording electrode. For each segment of data, the production of a smooth growth function with this method is evidence for a normal distribution of events (Barlow, 1990). In this case the 50% point represents the median inter-event interval.

Computer simulations

Computer simulations were performed using the simplified one compartment model of a TC neurone fully described in Tóth & Crunelli (1992). Briefly, the model consisted of I_T, I_h, a leak K^+ current (I_{Leak}) and the currents underlying the action potentials, (I_{Na} and I_{KD} – delayed rectifier). I_{Na} and I_{KD} were adapted from Traub, Wong, Miles & Michelson (1991). The equation used to describe the balance of transmembrane currents is:

$$C_m(dV/dt) = -(I_T + I_h + I_{KD} + I_{Na} + I_{Leak}) + I_{inj},$$

where C_m (= 50 pF) is the membrane capacitance, and I_{inj} is the injected current. All kinetic data are given for a temperature of 35 °C. The equations used to describe I_T are:

$$I_T = g_T m_{Ca}{}^3 h_{Ca}(V - E_{Ca}),$$

$$m_{Ca\infty} = 1/[1 + \exp(-(V + 63)/7{\cdot}8)],$$

$$h_{Ca\infty} = 1/[1 + \exp((V + 83{\cdot}5)/6{\cdot}3)],$$

$$\tau_{mCa} = 2{\cdot}44 + 0{\cdot}02506\exp(-0{\cdot}0984 \times V),$$

$$\tau_{hCa} = 7{\cdot}66 + 0{\cdot}02868\exp(-0{\cdot}1054 \times V),$$

where E_{Ca} = 180 mV, g_{Ca} varied between 30 and 70 nS.

The equations used to describe I_h are:

$$I_h = g_h m_h{}^3(V - E_h),$$

$$m_{h\infty} = 1/[1 + \exp((V + 75)/5{\cdot}5)],$$

$$\tau_{mh} = 120820/\exp(0{\cdot}061 \times V), \text{for } V > -77{\cdot}5 \text{ mV},$$

$$\tau_{mh} = 29{\cdot}54/\exp(-0{\cdot}046 \times V), \text{for } V \leqslant -77{\cdot}5 \text{ mV},$$

where E_h = −33 mV, g_h varied between 0 and 24 nS.

The equation used to describe the leakage current I_{Leak} is:

$$I_{Leak} = g_{Leak}(V - E_{Leak}),$$

where E_{Leak} = −95 mV, g_{Leak} varied between 1·7 and 12·5 nS.

In the above equations, m_{Ca} and m_h are the activation variables of I_T and I_h, respectively, h_{Ca} is the inactivation variable of I_T. Each of these obey the differential equation:

$$dy/dt = (y_\infty - y)/\tau_y,$$

where $y = m_{Ca}$, m_h or h_{Ca}.

Accordingly, y_∞ represents the steady-state values of the activation and inactivation variables (m_{Ca}, m_h and h_{Ca}) given above, and τ_y the corresponding time constants. $g_{T,max}$, g_h and g_{Leak} are the maximal conductances of I_T, I_h and I_{Leak}, respectively, while E_{Ca}, E_h and E_{Leak} are the corresponding reversal potentials.

The system of differential equations was integrated using a slightly modified version of the fourth order Runge–Kutta method with a constant step size of 0·1 ms or an adaptive step size (Tóth & Crunelli, 1992).

RESULTS

Electrophysiological recordings

During the course of the studies in the cat ventrobasal thalamus described in the accompanying papers (Turner *et al.* 1997; Williams, Turner, Hughes & Crunelli, 1997) and previous investigations in the rat and cat dorsal lateral geniculate nucleus (Turner *et al.* 1994; Williams *et al.* 1996), we have recorded twenty-eight of 189 TC neurones that demonstrated novel non-linear membrane properties that were apparent at membrane potentials centred around −60 mV. In these neurones voltage responses evoked by small amplitude (10–50 pA) negative current steps showed a multiphase decay process, and were characterized by a time-dependent increase in input resistance (Fig. 1*A*). Analysis of voltage–current (*V–I*) relationships revealed that in a voltage range around −60 to −65 mV such neurones possessed slope conductance values of less than 1 nS, indicating an apparent input resistance in the gigaohm range (Figs 1–4). This phenomenon was highly dependent upon the holding potential of the neurone, so that from a potential more positive than −60 mV responses to small negative current steps could be described as almost electrotonic in nature, whilst from holding potentials around −60 to −65 mV they displayed a time-dependent increase in input resistance (Fig. 1*B*). When challenged with relatively small, short current steps, this non-linear membrane behaviour gave rise to amplification not only in the voltage but also in the time domain, so that voltage responses could outlast the injected current steps by up to ten times. These voltage responses were invariably terminated by a LTCP and burst firing of action potentials (Fig. 2*A* and *B*). This behaviour is hereafter referred to as input signal amplification. Plots of the duration of the voltage responses (calculated as the time taken for the neurone to fire an action potential) against the duration of the negative current step, revealed characteristic input–output relationships, with non-linear and linear components (Fig. 2*Bc*) ($n = 5$ neurones), and clearly indicated that the non-linear component was, in the main, apparent when negative current steps were of relatively short duration and small amplitude. A similar phenomenon could also be evoked at the offset of voltage responses evoked by positive current steps, but only when the holding potential was set more negative than −60 mV (Fig. 2*C*), indicating that input signal amplification could only be formed if the membrane potential was passed across an apparent threshold voltage of −60 to −65 mV from an initial value more positive than this range.

The intrinsic nature of input signal amplification was verified by resistance to the application of tetrodotoxin (1 μM) ($n = 4$) (Fig. 3*B*) and excitatory and inhibitory amino acid receptor antagonists ($n = 9$) (Figs 1, 2 and 3*B*). Furthermore, these data demonstrated that input signal amplification was not dependent upon the activation of Na^+

currents. As input signal amplification gave rise to hyperpolarizing voltage responses we investigated whether the mechanisms responsible for its generation involved hyperpolarization-activated membrane currents such as I_h or the inwardly rectifying K^+ current (I_{KIR}) described in the accompanying paper (Williams *et al.* 1997). As shown in Fig. 3*A*, input signal amplification was resistant to the application of the specific I_h antagonist ZD 7288 (100–300 μM) ($n = 6$) (Harris & Constanti, 1995; Williams *et al.* 1997), although the block of I_h led to the formation of membrane bistability (see below) (Fig. 8). The I_{KIR} channel blocker Ba^{2+} (0·1–2·0 mM) abolished fast rectification of negative voltage responses (compare Fig. 3*B* with 3*A* and 4*A*) (cf. Williams *et al.* 1997), but failed to block input signal amplification ($n = 2$) (Fig. 3*B*). In TC neurones that did not exhibit input signal amplification under control conditions, the application of Ba^{2+} led to the unmasking of this behaviour ($n = 2$), a property that may have resulted from a voltage- and time-dependent blockade of I_{KIR} (Uchimura, Cherubini & North, 1989). We suggest that this is not the

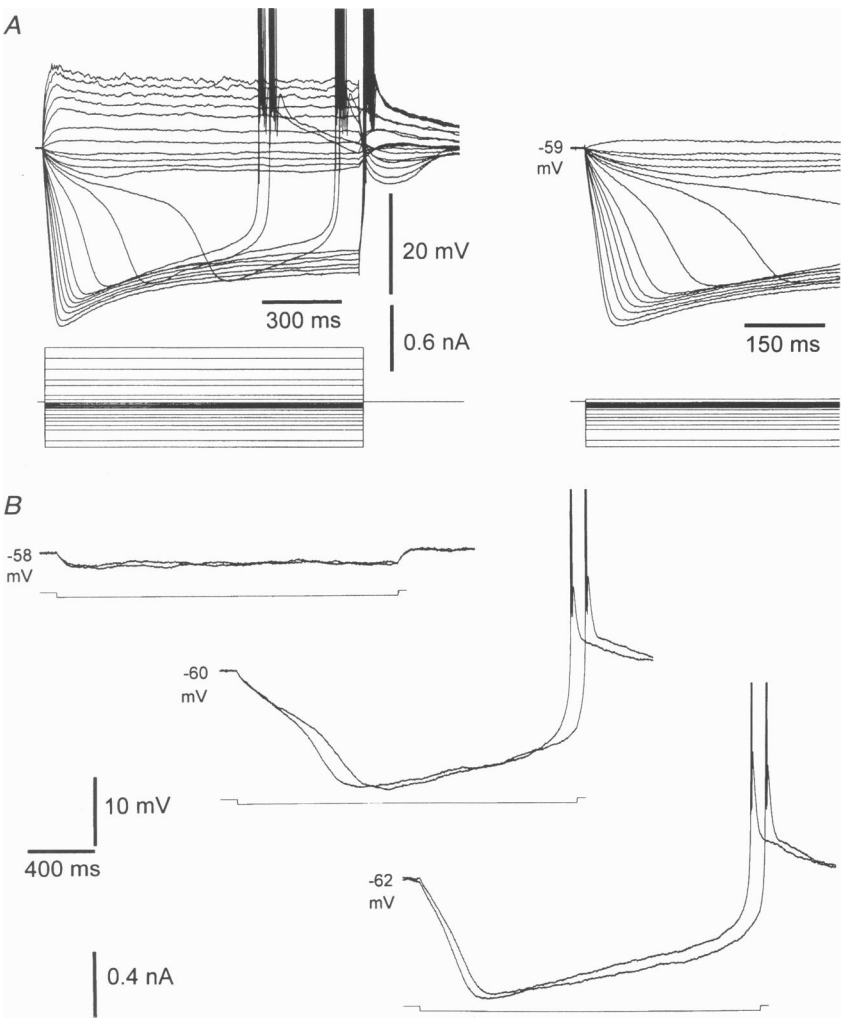

Figure 1. Time-dependent increase in the apparent input resistance of TC neurones

A, superimposed families of voltage responses (upper traces) and current steps (lower traces) demonstrate the non-linear structure of the voltage–current relationship in a TC neurone of the cat ventrobasal thalamus. The four smallest (< −50 pA) negative current steps gave rise to voltage responses of a conventional structure. Larger negative current steps, however, evoked voltage responses of large amplitude and demonstrated a time-dependent increase in input resistance. The structure of the voltage responses is shown on a faster time base to the right of the figure. Note that the time taken for the voltage responses to reach the most negative potential was dependent upon the value of the current step. *B*, a similar response pattern was evoked by negative current steps in another TC neurone of the cat ventrobasal thalamus. Voltage responses ($n = 2$ traces) are shown at three values of membrane potential (indicated to the left of the traces). At the two most negative membrane potentials large amplitude, hyperpolarizing voltage responses characterized by a time-dependent increase in input resistance were evoked. Records in *A* and *B* were obtained in the presence of APV (100 μM), CNQX (20 μM), bicuculline (30 μM) and CGP 35348 (500 μM). The amplitude of action potentials has been truncated for clarity.

case, as the voltage- and time-dependent blockade of I_{KIR} in TC neurones is first apparent at membrane potentials more negative than −85 mV (Williams *et al.* 1997), some 20 mV more negative than the range where input signal amplification is manifest. Furthermore, under voltage clamp conditions the current–voltage relationships of TC neurones that exhibit input signal amplification revealed that current responses lacked any form of time dependence that mimicked the time-dependent increase in input resistance observed under current clamp conditions ($n = 3$) (Fig. 4). We, therefore, suggest that input signal amplification does not involve the deactivation of I_h and I_{KIR}, and that the unmasking of input signal amplification by Ba^{2+} results from a decrease in the neurone input conductance (see below).

A decrease in $[Ca^{2+}]_o$ (from 2 to 1 mM) and an increase in $[Mg^{2+}]_o$ (from 1 to 10 mM), a procedure known to reduce the amplitude of Ca^{2+} currents in TC neurones (Crunelli *et al.* 1989), however, blocked input signal amplification ($n = 3$) (Fig. 3*C*). Similarly, the application of the Ca^{2+} current antagonist Ni^{2+} (2–3 mM) ($n = 2$) (Coulter *et al.* 1989; Crunelli *et al.* 1989; Hernandez-Cruz & Pape, 1989; Huguenard, 1996) blocked input signal amplification (not illustrated). Perfusion with a low Ca^{2+}, high Mg^{2+} medium or addition of Ni^{2+} could be accompanied by a small hyper-

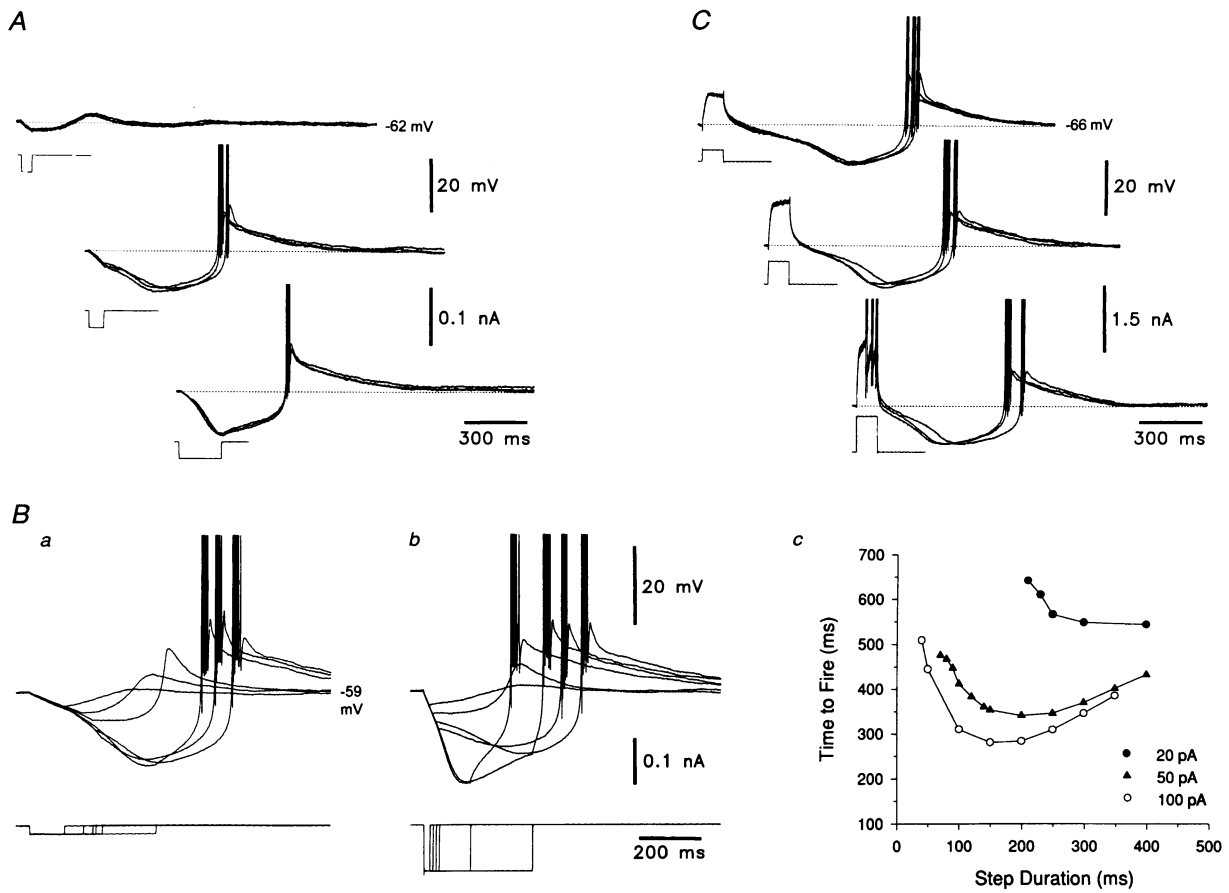

Figure 2. Properties of input signal amplification in TC neurones

A, short negative current steps (indicated below the main traces) generated large amplitude hyperpolarizations that greatly outlasted the duration of the input steps and lead to input signal amplification in both the voltage and time domains. *B*, voltage responses (upper traces) to −20 (*a*) and −100 pA (*b*) current steps (lower traces) of different durations, as used to investigate the degree of input signal amplification. In *Ba* note how the voltage responses evoked by the four longest current steps are much longer than the input signals. This non-linear relationship between the duration of the current step and the interval between the onset of the current step and the time to fire an action potential is further illustrated by the representative graph in *Bc*, for the three indicated values of injected current. Note that the shortest (around 50 ms) current steps gave rise to an action potential output 500 ms after the beginning of the input signal. *C*, another TC neurone, recorded in the presence of APV (100 μM), CNQX (20 μM), bicuculline (30 μM) and CGP 35348 (500 μM), exhibited input signal amplification at the offset of positive current steps. Voltage traces ($n = 3$ traces) evoked by positive current steps of three different amplitudes (lower traces) demonstrate that the duration of the hyperpolarizing voltage responses is inversely related to the amplitude of the injected current steps. Traces in *A*, *B* and *C* are from three TC neurones in the cat ventrobasal thalamus, and the amplitude of action potentials has been truncated for clarity.

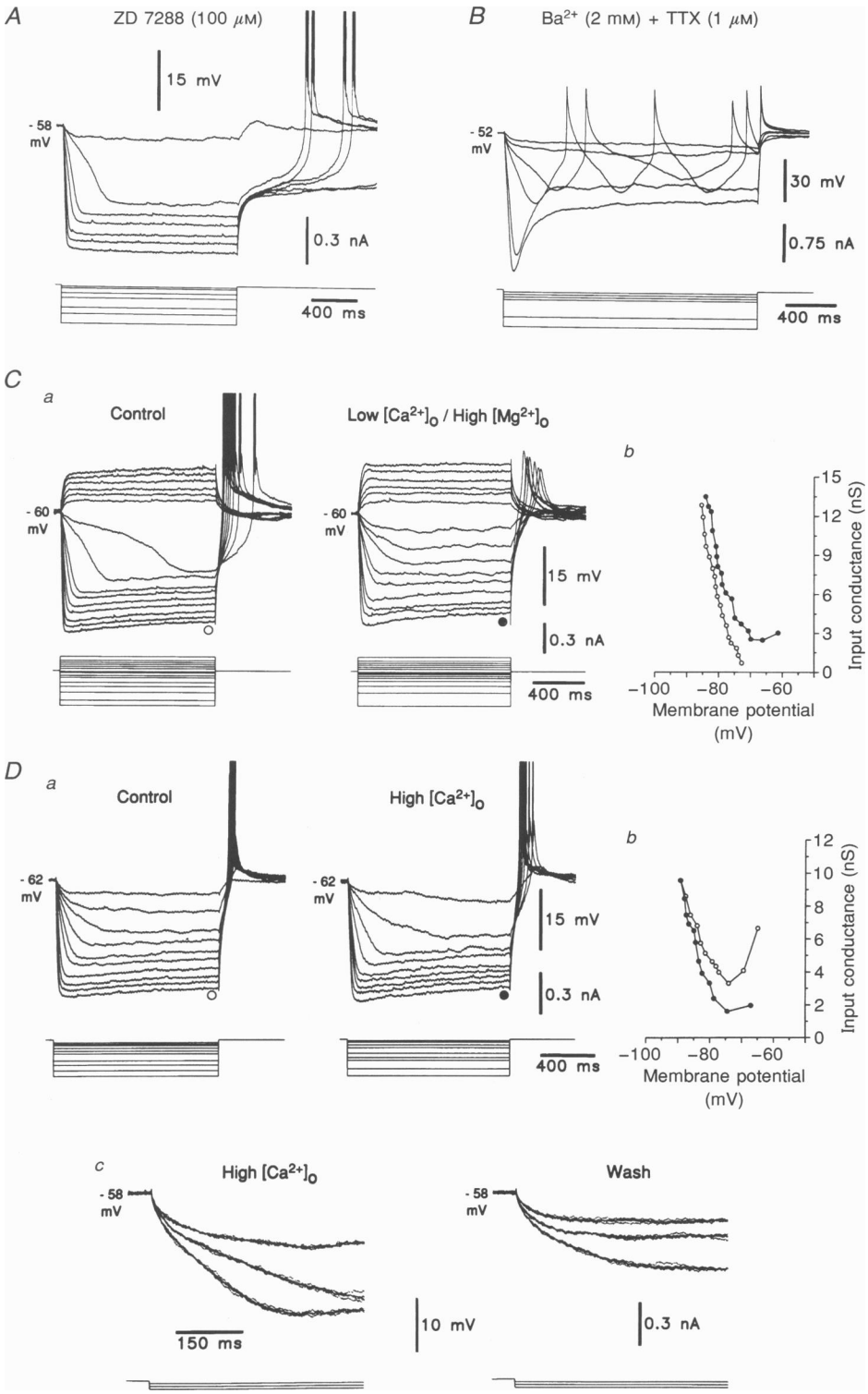

Figure 3. Ionic basis of input signal amplification

A, the generation of input signal amplification was resistant to the blockade of I_h. In a TC neurone of the rat dorsal lateral geniculate nucleus recorded in the presence of ZD 7288 (100 μM), voltage responses (upper traces) evoked by steps of injected current (lower traces) demonstrated input signal amplification, if a critical membrane potential range was entered. The amplitudes of voltage responses evoked by the two smallest negative current steps were separated by more than 15 mV (see also Fig. 8*A*). *B*, the pharmacological blockade of Na^+ and K^+ currents did not block input signal amplification in a TC neurone of the cat ventrobasal thalamus. Voltage responses (upper traces) evoked by steps of negative current (lower

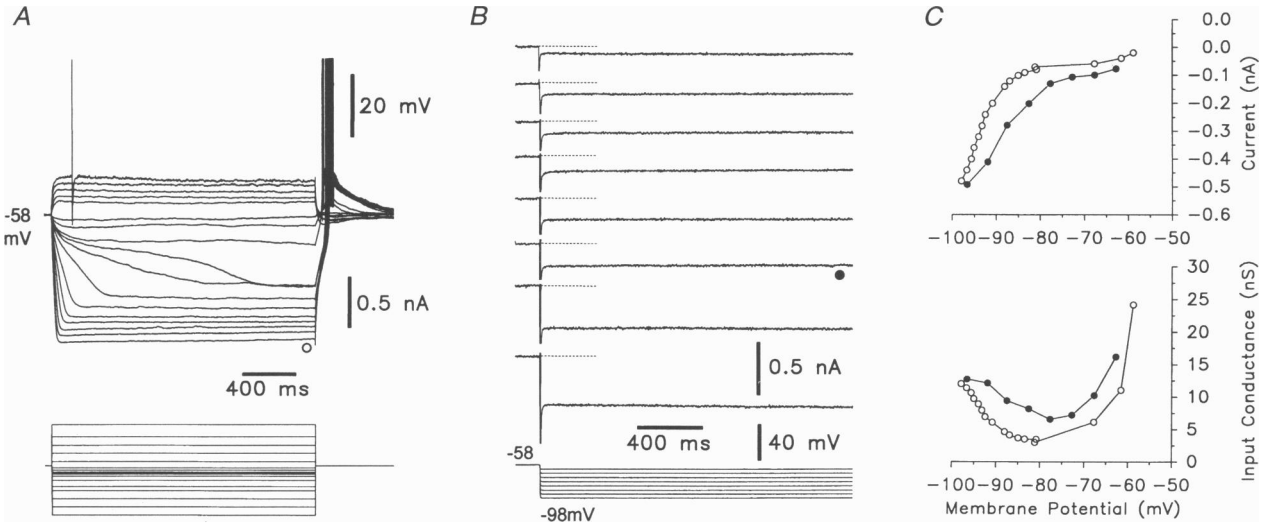

Figure 4. Non-linear, steady-state current–voltage relationships recorded under current- and voltage clamp conditions

A, under current clamp conditions the superimposition of families of voltage responses (upper traces) demonstrated input signal amplification, marked by the presence of negative voltage responses that exhibit a time-dependent increase in input resistance. *B*, under voltage clamp conditions, current records (upper traces) from the same TC neurone of the cat ventrobasal thalamus as in *A* did not reflect the time-dependent nature of the voltage responses recorded under current clamp conditions. This neurone was recorded in the presence of ZD 7288 (300 μM), consequently no depolarizing sag was apparent during the course of negative voltage responses, or any time-dependent inward current under voltage clamp conditions. *C*, the upper graph displays the steady-state current–voltage relationship recorded under current- (○) and voltage clamp (●) conditions. Note the non-linear structure of this relationship. The lower graph illustrates a plot of the input conductance against membrane potential, under both recording conditions. Note that these relationships have a similar structure. The amplitude of action potentials has been truncated for clarity.

traces) showed input signal amplification, marked by a time-dependent increase in input resistance. Note that the two smallest voltage responses did not reach the membrane potential range for input amplification (cf. Fig. 9). The absence of action potentials indicates the blockade of Na^+ currents with tetrodotoxin (TTX, 1 μM). The blockade of K^+ currents by Ba^{2+} (2 mM) is demonstrated by the absence of fast anomalous rectification (cf. Williams *et al.* 1997), so that, for example, a current pulse of −0·5 nA would produce a voltage response greater than 50 mV (compare with *A* and *C*). Note that this neurone could produce the novel type of oscillation (cf. Fig. 7*A*), as indicated by the long shoulder of the LTCP present during some of the hyperpolarizing responses. *C*, input signal amplification was abolished by the reduction of a Ca^{2+} current. Under control conditions this rat neurone showed input signal amplification (*Ca*, left panel). The reduction of $[Ca^{2+}]_o$ from 2 to 1 mM and the increase of $[Mg^{2+}]_o$ from 1 to 10 mM abolished this phenomenon (*Ca*, right panel), as indicated by the absence of a time-dependent increase in input resistance, and by the increase of the input conductance of the neurone over the potential range −60 to −80 mV (○, control; ●, low $[Ca^{2+}]_o$ high $[Mg^{2+}]_o$) (*Cb*). The reduction of I_T is inferred by the decrease in the amplitude of the LTCPs that could no longer reach firing threshold. *D*, input signal amplification was formed *de novo* by an increase in $[Ca^{2+}]_o$. Under control conditions this neurone did not exhibit input signal amplification (*Da*). An increase in the $[Ca^{2+}]_o$ from 2 to 8 mM, however, lead to the formation of voltage responses that showed a time-dependent increase in input resistance. These effects are illustrated in *Db*, where the increase in $[Ca^{2+}]_o$ (●) is clearly seen to lead to a decrease in input conductance over a voltage range of −60 to −80 mV. *Dc*, the effects of increasing $[Ca^{2+}]_o$ were reversible. In the same neurone as shown in *Da* and *Db*, but from a more positive membrane potential, responses ($n = 3$ dotted lines) evoked in the presence of high $[Ca^{2+}]_o$ demonstrated a time-dependent increase in input resistance (the continuous line is the average of the dotted traces). The reduction of $[Ca^{2+}]_o$ to the control value normalized the charging of the neurone. Traces in *C* and *D* were recorded from two TC neurones of the rat dorsal lateral geniculate nucleus, and the amplitude of action potentials has been truncated for clarity.

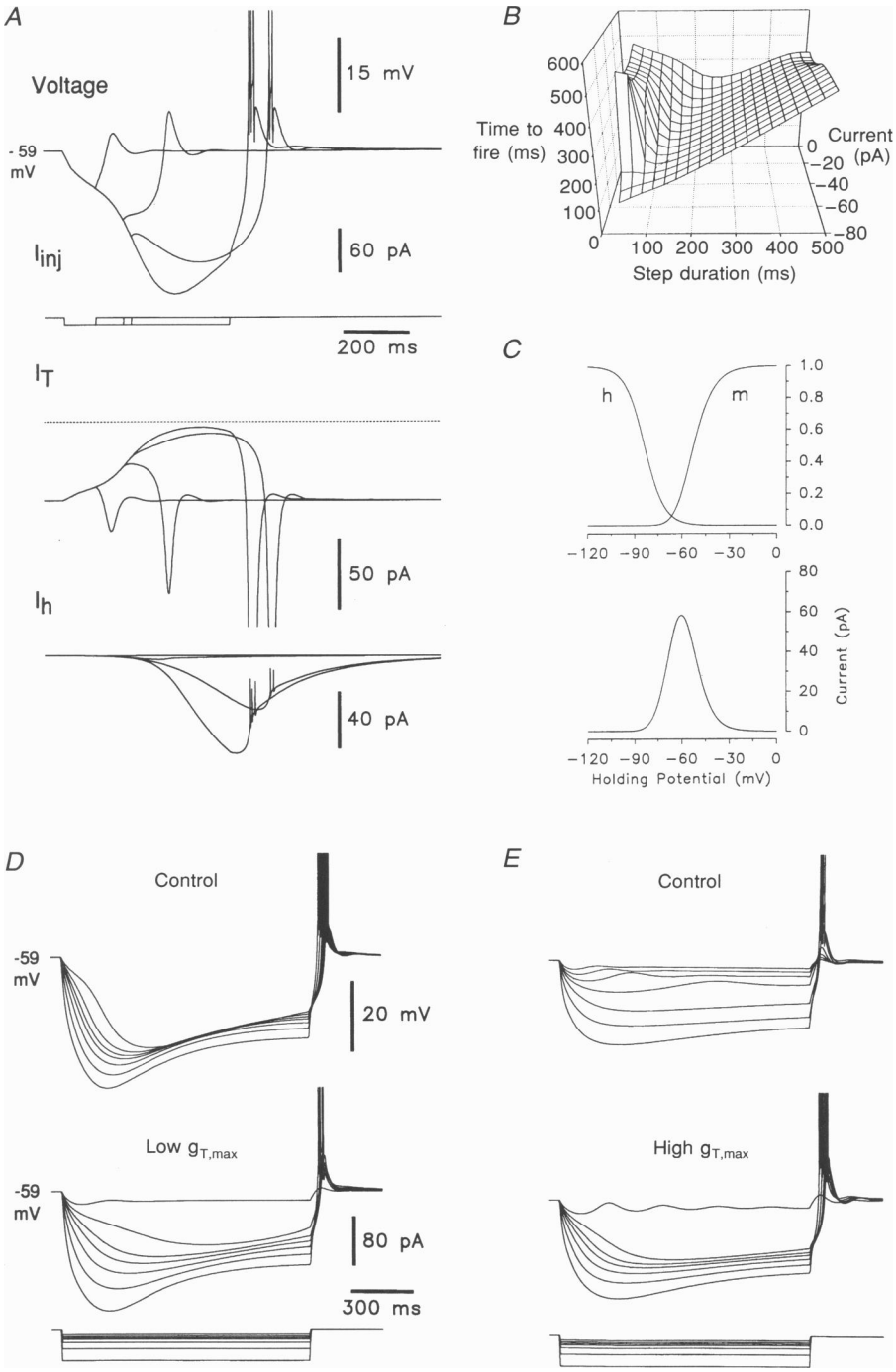

Figure 5. Computer simulation of input signal amplification

A, simulated voltage responses, evoked by pulses of negative injected current (I_{inj}) from a membrane potential of −59 mV, greatly outlasted the current steps. Note the similarity of the simulations compared with the experimental records shown in Fig. 2*Bb*. Simultaneous analysis of I_T and I_h, indicates that at this membrane potential a steady (window) component of I_T is apparent ($g_{T,max}$, 49·2 nS; g_h, 24 nS; g_{Leak}, 2 nS). In response to negative current steps, window I_T decreased to approach zero (dashed line) in a time-dependent manner. The time course of I_T paralleled the early portion of the voltage responses, whilst activation of I_h was delayed. As the membrane potential became more negative, I_h was activated leading to depolarization. Depolarization caused a large transient activation of I_T, which then settled to the pre-step level (window component). *B*, this graph illustrates the non-linear relationship between the duration of current steps of different sizes and the interval between the onset of the current step and the time to fire an action potential, obtained from a series of simulations similar to those shown in *A*. Note the similarity with the plot derived from the experimental data (Fig. 2*Bc*), and in particular that the shortest (around 50 ms) current steps give rise to a more than ten times amplification of the duration of the input signal. *C*, a

polarization (2–3 mV) or outward current (20–50 pA), under current- and voltage clamp conditions, respectively, that were at the limit of resolution of the two techniques. An increase in $[Ca^{2+}]_o$ (from 2 to 8 mM) ($n = 3$) produced properties reminiscent of input signal amplification in neurones that under control conditions did not show this behaviour (Fig. 3*D*). These results, therefore, demonstrate that input signal amplification is dependent upon the influence of a Ca^{2+} current. Specifically, we suggest that the low threshold Ca^{2+} current (I_T) plays a crucial role in the formation of input amplification, as other Ca^{2+} currents expressed by TC neurones are activated from membrane potentials more positive than −40 mV (Hernandez-Cruz & Pape, 1989; Guyon & Leresche, 1996).

Computer simulations

We reproduced input signal amplification with a simplified model of a TC neurone, that contained the membrane currents I_T, I_h, I_{Na}, I_{KD} and I_{Leak}. (Note that I_{Na} and I_{KD} were only required to reproduce the action potentials and were not essential for simulating the basic voltage waveform of input signal amplification.) The model, originally constructed to reproduce the intrinsic pacemaker (or delta) oscillation in TC neurones (Tóth & Crunelli, 1992), was found to exhibit input signal amplification when the K^+ leak conductance (g_{Leak}) was reduced to a value of less than 2 nS; no other parameter change was required to simulate this activity. Thus, in response to small negative current steps the model accurately reproduced the waveform of input signal amplification and its associated time-dependent increase in input resistance (Fig. 5*A*) that were observed experimentally (Figs 1 and 2). In addition, a close quantitative correspondence between the experimental results and the simulations could be achieved with respect to the time required to generate an action potential output (compare Figs 5*B* and 2*Bc*).

The simultaneous analysis of the simulated membrane voltage and currents revealed a steady component of I_T with an amplitude of about 50 pA at a holding potential of −59 mV (Fig. 5*A*). During the voltage responses that showed the time-dependent increase in input resistance the amplitude of this component of I_T decreased concurrently with the membrane potential, whilst I_h was steady and only later contributed to the membrane potential response (Fig. 5*A*). We propose that this steady component of I_T represents a window current, and, as the steady-state activation and inactivation curves of I_T (Fig. 5*C*) were obtained from the results of previous experiments (Coulter *et al.* 1989; Crunelli *et al.* 1989), it appears that this window current underlies input signal amplification in TC neurones. Window I_T has a steep voltage dependence (Fig. 5*C*, lower graph), so that at a holding potential of around −60 mV this inward current is maximal, but decreases exponentially with membrane depolarization or hyperpolarization. The similarity between the voltage at which window I_T is near maximal and the apparent threshold for the generation of input signal amplification described in the experiments is striking.

To test the involvement of window I_T in the formation of input signal amplification we manipulated the maximal conductance of I_T ($g_{T,max}$) in order to scale the value of window I_T. In simulations with a value of g_{Leak} of 2 nS or less, a reduction of $g_{T,max}$ from 49 to 30 nS abolished input signal amplification (Fig. 5*D*). When g_{Leak} was increased to 3 nS amplification properties were not apparent, but an increase of $g_{T,max}$ from 49 to 70 nS led to their re-appearance (Fig. 5*E*). These results, therefore, demonstrated that the formation of input signal amplification not only requires window I_T but is also dependent upon the ratio of $g_{T,max}$ and g_{Leak} rather than upon their absolute values.

Physiological expression of input signal amplification

Input signal amplification was also found to occur in the absence of injected current steps (Fig. 6). Firstly, small spontaneous oscillations of the membrane potential present in TC neurones at around −60 mV were able to trigger large amplitude hyperpolarizations that were terminated by a LTCP and action potentials when the holding potential was set at around −60 mV ($n = 6$) (Fig. 6*A*). Secondly, in all of five neurones tested, pharmacologically isolated single EPSPs ($n = 3$) (Fig. 6*Ba*) or $GABA_B$ receptor-mediated IPSPs ($n = 2$) (Fig. 6*Ca*) gave rise to long duration, large amplitude, hyperpolarizing voltage responses terminated by the burst firing of action potentials, when the holding potential was in the range −60 to −65 mV. Thus, spontaneous oscillations, as well as evoked excitatory and inhibitory postsynaptic potentials, can be amplified in the voltage and time domains, demonstrating that input signal amplification can be triggered by physiologically relevant stimuli and that it is not an artifactual product of the current injection system.

Our simplified TC neurone model also reproduced the ability of synaptic inputs to generate input signal amplification. In response to small amplitude EPSPs or IPSPs, simulated using a double exponential function, long lasting hyperpolarizing voltage responses, terminated by a LTCP and burst firing of action potentials, were evoked at a holding

voltage overlap between the third power of the activation curve (m) and the inactivation (h) curve of I_T (upper graph), as described by previous studies (Coulter *et al.* 1989; Crunelli *et al.* 1989), forms the basis of window I_T (lower graph). *D*, a reduction of $g_{T,max}$ from 49·2 (control traces) to 30 nS (low $g_{T,max}$ traces) abolishes input signal amplification (g_{Leak}, 1·7 nS; g_h, 2 nS). *E*, when g_{Leak} was increased to 3 nS amplification properties were not apparent (control traces), but an increase of $g_{T,max}$ from 49 to 70 nS led to their re-appearance. The amplitude of I_T (in *A*) and of action potentials has been truncated for clarity.

potential of around −60 mV when an appropriate ratio between $g_{T,max}$ and g_{Leak} was used (Fig. 6*Bb* and *Cb*).

Oscillatory activity

Intrinsic, low frequency (0·5–4 Hz) oscillatory activity, termed pacemaker or delta oscillation and characterized by the cyclical generation of LTCPs crowned by the burst firing of action potentials, has been described in TC neurones maintained *in vivo* and *in vitro* (McCormick & Pape, 1990; Leresche *et al.* 1991; Steriade *et al.* 1993). In TC neurones that exhibited input signal amplification a novel pattern of intrinsic, low frequency oscillatory activity was apparent (Fig. 7*A*). This novel oscillation was similar to the delta oscillation in that it existed only within a limited voltage range and was insensitive to tetrodotoxin (1 μM) (cf. Fig. 3*B*) and to excitatory and inhibitory amino acid receptor antagonists ($n = 8$) (Fig. 7*A*). It differed from the delta oscillation, however, in three features. Firstly, at its upper voltage limit of existence the novel oscillation showed a long plateau in each LTCP (Fig. 7*A*) which was terminated by a large negative membrane potential excursion and which was similar in structure to the hyperpolarizing voltage response evoked by a small negative current step (cf. Figs 1 and 2). At its lower voltage limit of existence, LTCPs were found to

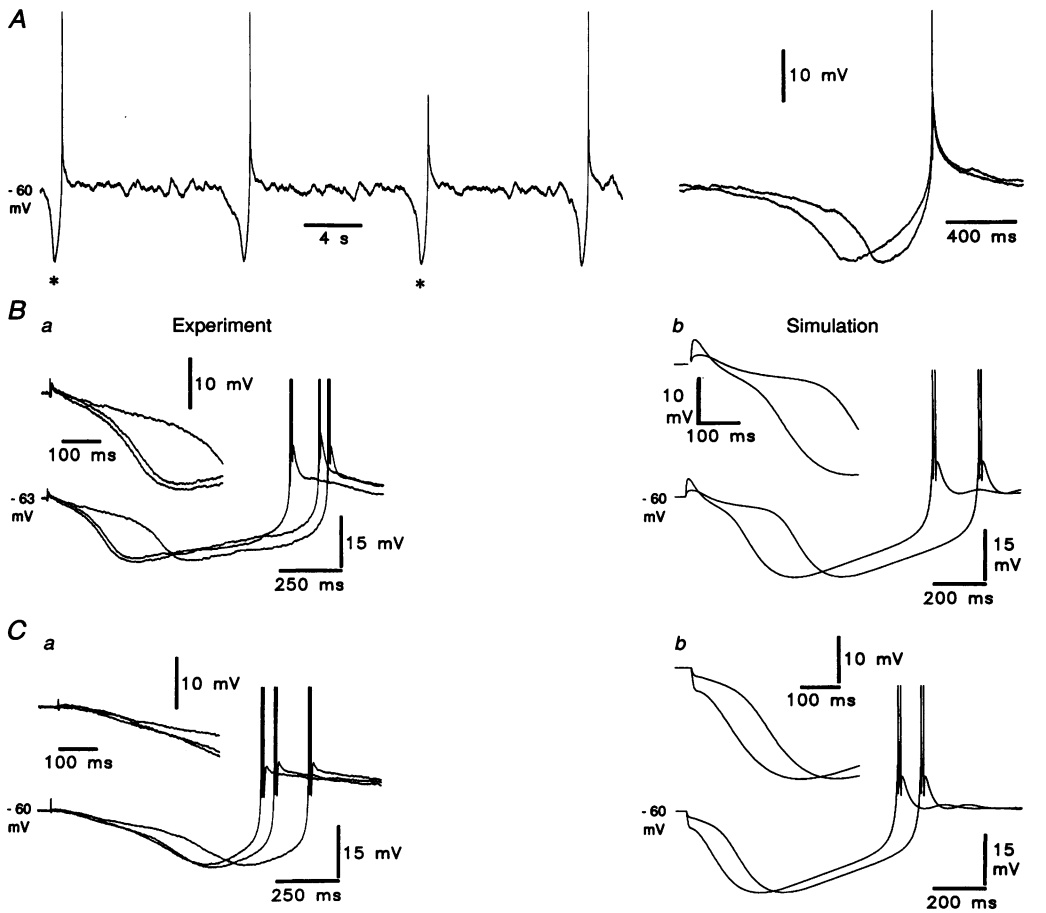

Figure 6. Input signal amplification can occur in response to spontaneous membrane potential oscillations and synaptic potentials

A, voltage records from a TC neurone of the rat dorsal lateral geniculate nucleus show small oscillations of the membrane potential giving rise to large amplitude, long lasting hyperpolarizations terminated by a LTCP that could be crowned by the firing of an action potential. The regularity of these events, two of which (*) are shown on a faster time base to the right of the figure, was observed in every neurone showing this behaviour. *Ba*, single EPSPs ($n = 3$ traces), elicited by electrical stimulation of the optic tract, evoked large hyperpolarizing voltage responses in a cat TC neurone of the dorsal lateral geniculate nucleus, recorded in the presence of bicuculline (30 μM) and CGP 35348 (500 μM). The variability between responses evoked by the same intensity of stimulation is shown on a faster time base. *Ca*, single $GABA_B$ receptor-mediated IPSPs ($n = 3$ traces), evoked by direct electrical stimulation of the nucleus reticularis thalami, gave rise to similar responses in a cat TC neurone of the ventrobasal thalamus, recorded in the presence of APV (100 μM), CNQX (20 μM) and bicuculline (30 μM). The initial period of the response is shown on a faster time base. *Bb* and *Cb*, simulated EPSPs and $GABA_A$ IPSPs, respectively, can induce a pattern of input signal amplification similar to those observed experimentally. The amplitude of action potentials has been truncated for clarity.

lack plateau components (Fig. 7*A*). Indeed, a progression in the shape of LTCPs took place as the neurone was hyperpolarized by changes in the DC injection (not illustrated). Secondly, at the upper voltage limit of existence the novel oscillation had bursts of action potentials superimposed upon LTCPs (Fig. 7*A*), while they are absent in the delta oscillations (cf. Fig. 1 in Leresche *et al.* 1991; and Fig. 1 in Antal, Emri, Tóth & Crunelli, 1996). Thirdly, the relationship between the oscillation frequency and the injected DC was different in the two oscillatory types.

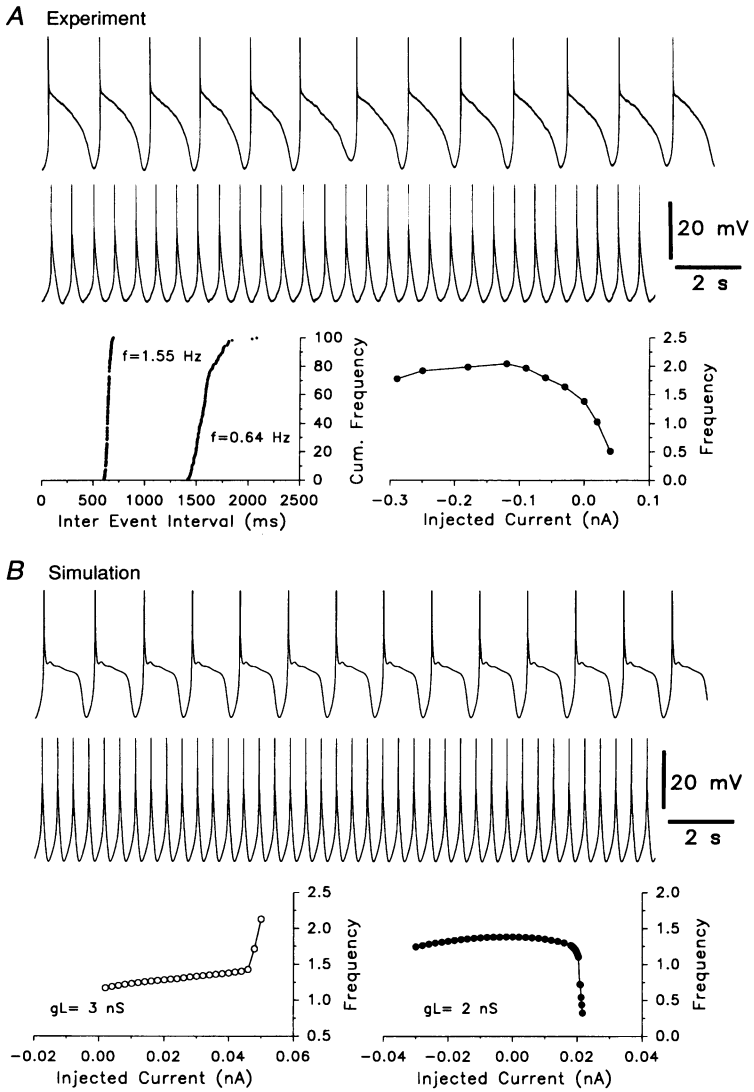

Figure 7. The novel type of intrinsic low frequency oscillatory activity of TC neurones

A, voltage records illustrate the novel type of oscillatory activity at its upper and lower voltage limits of existence (upper and lower records, respectively) in a TC neurone of the cat ventrobasal thalamus, that demonstrated input signal amplification. The left graph shows the cumulative integrative frequency of inter-event intervals (see Methods) for the oscillation depicted in the upper and lower traces (right and left curves, respectively). For a different neurone the dependence of oscillation frequency upon the value of DC injected through the recording electrode is shown in the right graph. Note that the frequency first increased and then decreased with increasing values of DC. The most negative potential reached by the oscillation was −77 and −75 mV in the upper and lower trace, respectively. These neurones were recorded in the presence of APV (100 μM), CNQX (20 μM), bicuculline (30 μM) and CGP 35348 (500 μM). *B*, oscillatory activity of the model neurone. The upper and lower traces show the simulated oscillation obtained at its upper and lower voltage limit of existence, and demonstrate a close correspondence with the experimental records ($g_{T,max}$, 49 nS; g_h, 24 nS; g_{Leak}, 2 nS). The graphs below illustrate the existence of two qualitatively different relationships between the frequency and the injected DC during the novel oscillation (right graph) and the delta oscillation (left graph); they can be transformed into each other by changing the value of g_{Leak} (gL). The most negative potential reached by the oscillation was −80 and −79 mV in the upper and lower traces, respectively. The amplitude of action potentials in simulations and experimental records has been truncated for clarity.

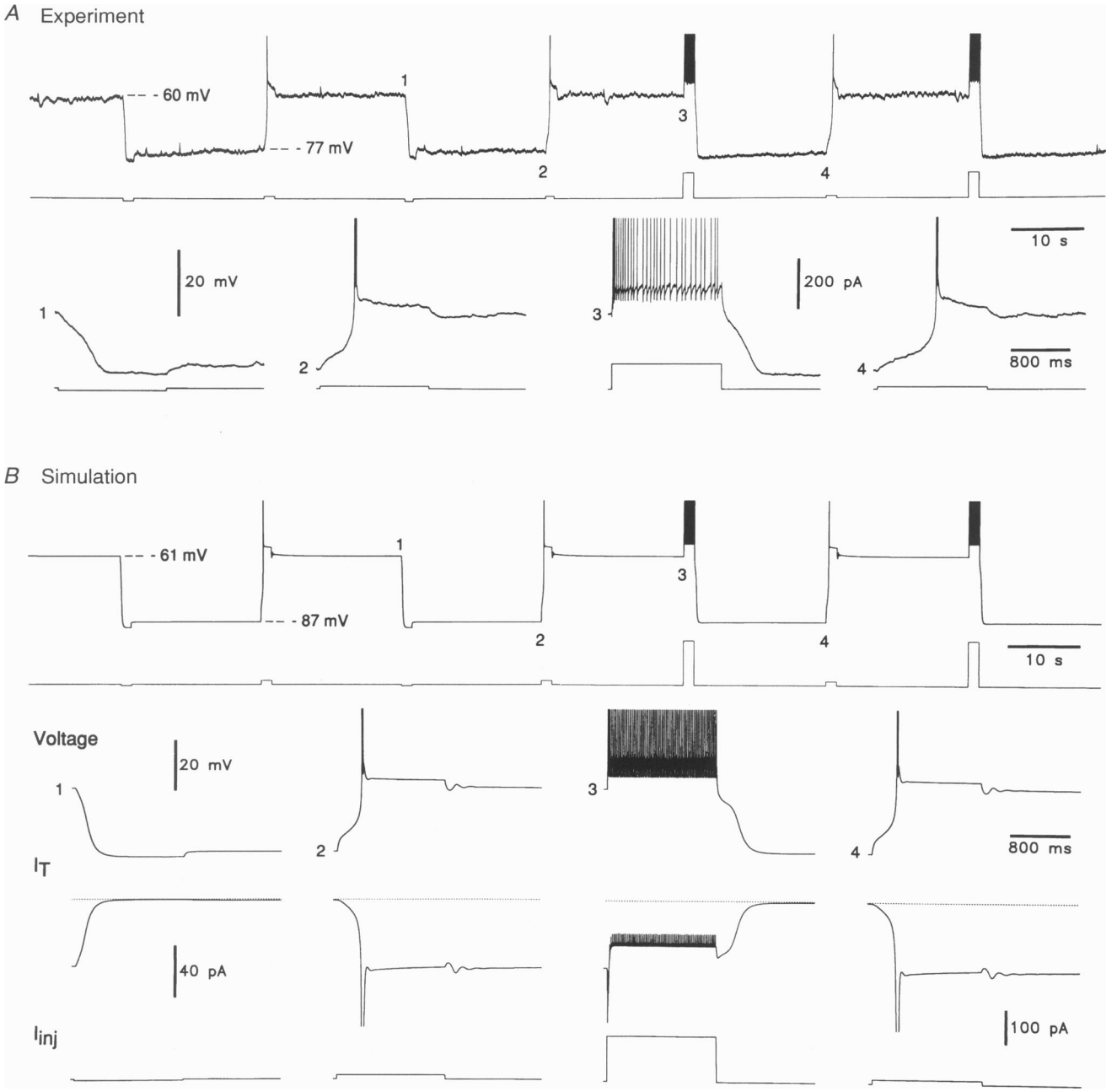

Figure 8. Intrinsic bistability of TC neurones

A, bistable behaviour of a TC neurone in the rat dorsal lateral geniculate nucleus following the blockade of I_h with ZD 7288 (100 μM). The neurone exhibited two stable resting membrane potentials (equilibrium potentials) (upper continuous trace). Transition between equilibrium potentials was evoked by relatively short steps of positive or negative injected current, superimposed on a 70 pA DC (lower continuous trace). The membrane potential and the injected current steps at four (numbered) transition points are shown on a faster time base in the lower traces. At transition point 1, the membrane rested at the more positive equilibrium potential and was then switched to the more negative equilibrium potential upon termination of a −10 pA current step. Transition from the more negative to the more positive equilibrium potential took place upon the termination of a 10 pA current step (transition point 2). Under these conditions, therefore, large amplitude voltage responses may be evoked by pulses of positive current. Voltage responses at transition points demonstrated a time-dependent increase in input resistance. *B*, computer simulations replicated the experimental records when g_h was set to zero. Voltage records (upper continuous trace), when $g_{T,max} = 49$ nS and $g_{Leak} = 1{\cdot}7$ nS, showed two stable resting potentials that were switched by current steps, superimposed on a 16 pA DC (lower continuous trace). The time course of voltage responses and I_T are shown at four (numbered) transition points (lower traces). At the more positive equilibrium potential

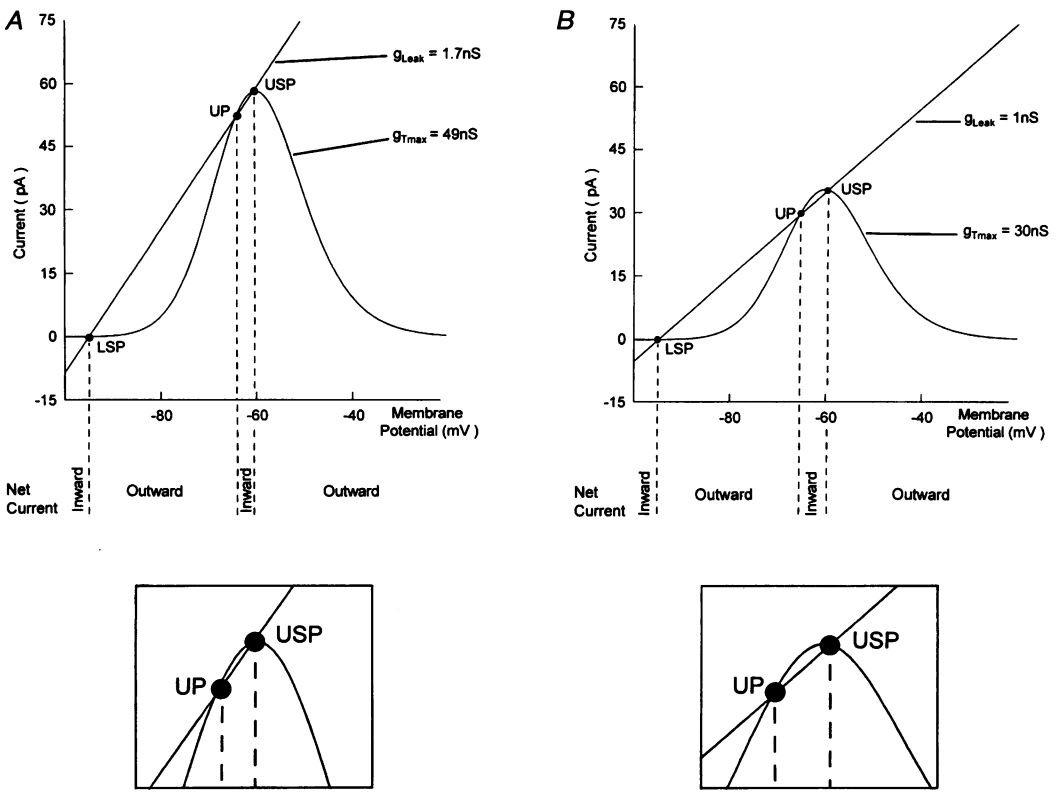

Figure 9. Window I_T and I_{Leak} underlie input signal amplification and bistability

A, plot of I_T and I_{Leak} *versus* membrane potential, constructed with those values of $g_{T,max}$ and g_{Leak} used in the simulations, indicates the presence of one unstable (UP), one upper stable (USP) and one lower stable (LSP) point where inward (I_T) and outward (I_{Leak}) current balance each other out. Voltage responses originating from USP, which will hyperpolarize the neurone to potentials less negative than that corresponding to UP, will be subjected to a net inward current that will re-instate the original stable point of current balance USP. Similarly, voltage responses originating from LSP, which will depolarize the neurone to potentials more negative than that corresponding to UP, will be subjected to a net outward current that will re-instate the original stable point of current balance LSP. However, negative voltage responses originating from USP will be amplified if they enter the voltage range between UP and LSP, since the net current in this range is outward, and the membrane potential will then settle at a value corresponding to USP. If $g_{T,max}$ is decreased to 30 nS while g_{Leak} is left unchanged (not shown), the net current over the entire voltage range will be outward, only one stable point of current balance will exist, and no input signal amplification or bistability can occur (cf. Fig. 5). *B*, a decrease of both $g_{T,max}$ and g_{Leak} to 30 and 1 nS, respectively, will, however, re-establish the presence of one unstable (UP) and two stable points (USP and LSP) of current balance. The lower plots in *A* and *B* are enlargements of the area around UP and USP.

Figure 7*A* illustrates voltage traces at the upper and lower limits of existence of the novel oscillatory activity, the corresponding cumulative integrative frequency plots of inter-event intervals (Fig. 7*A*, left graph) and the relationship between frequency of oscillation and different levels of injected DC (Fig. 7*A*, right graph). For the novel oscillation, the relationship between its frequency and the injected current described a complex pattern, characterized by an initial increase in frequency as the DC was made more negative, until a maximal point was reached; this was followed by a more subtle decrease in oscillation frequency. Note that the lowest frequency is achieved at the upper voltage limit of existence of the novel oscillation while in the delta oscillation the lowest frequency is present at the lower voltage limit of existence (cf. Fig. 1 in Leresche *et al.* 1991; and Fig. 1 in Antal *et al.* 1996).

(−61 mV), the window component of I_T was nearly maximal, while at the more negative equilibrium potential (−87 mV) it was negligible (zero level marked by dotted lines). The time course of voltage responses at transition points was mirrored by that of I_T, indicating that the voltage- and time-dependent removal of the window component of I_T underlies bistable behaviour. The amplitude of action potentials in simulations and experimental records has been truncated for clarity.

Figure 7*B* shows the computer simulations that reproduced this novel oscillatory activity. The close correspondence between simulation and experimental records is apparent from comparison of the traces obtained at the upper and lower voltage limits of existence and from the dependence of the frequency of activity upon the value of injected current (Fig. 7*B*, right graph). The novel pattern of oscillatory activity was found to be dependent upon the ratio of $g_{T,max}$ and g_{Leak}, in a manner identical to that of input signal amplification. Indeed, a transformation of the novel type of oscillation into the delta oscillation was produced by an increase of the value of g_{Leak} from 2 to 3 nS. Thus, in the presence of a value of g_{Leak} less than or equal to 2 nS a relationship between frequency and injected current (Fig. 7*B*, right graph) similar to that observed experimentally (Fig. 7*A*, right graph) for the novel oscillation was obtained, whilst an increase of g_{Leak} to values of at least 3 nS produced delta oscillation with its characteristic relationship between frequency and injected current (Fig. 7*B*, left graph). As the value of g_{Leak} was increased from 2 to 3 nS the plateau component of the LTCPs disappeared, indicating that for this novel oscillatory activity, as for input signal amplification, the functional expression of window I_T is dependent upon the balance of $g_{T,max}$ and g_{Leak}.

Bistable behaviour

Computer simulations also indicated that the duration of the large amplitude voltage responses elicited by small amplitude negative current steps were dependent upon the magnitude of the maximal conductance of I_h (g_h) (not illustrated). In experiments, the pharmacological blockade of I_h by application of ZD 7288 (100–300 μM) (Williams *et al.* 1997) led to the appearance of bistable behaviour ($n = 4$) (Fig. 8*A*), and similar results were obtained in simulations when the value of g_h was reduced to zero (Fig. 8*B*). In both cases, two stable equilibrium voltage levels separated by 15–30 mV were apparent. Transition between these equilibrium voltage levels was evoked by small and relatively brief current steps, so that in the experiment illustrated in Fig. 8*A*, for example, transition from the more positive to the more negative voltage level took place following the termination of a −10 pA step. It may be seen that in this neurone the charging of the membrane in response to this current step demonstrates a time-dependent increase in input resistance (Fig. 8*A*). It is also important to stress that (i) transition from the more positive to the more negative voltage level could be achieved by the use of both negative and positive current steps (Fig. 8*A*, traces 1 and 3) and (ii) under these conditions large amplitude voltage responses could be evoked from the more negative equilibrium voltage level by the application of small positive current steps (Fig. 8*A*, trace 4).

Identical results were obtained from the model neurone (Fig. 8*B*). The involvement of window I_T in the formation of the two stable voltage levels is illustrated by the fact that at the more positive voltage level the amplitude of window I_T is nearly maximal, whilst at the more negative voltage level the amplitude of window I_T approaches zero (Fig. 8*B*).

DISCUSSION

The main conclusions of this investigation are as follows. (i) TC neurones express intrinsic amplification properties which in a narrow membrane potential range centred around −60 mV enable EPSPs and IPSPs to give rise to a common output waveform, characterized by a large amplitude, long lasting hyperpolarization, that is invariably terminated by the burst firing of action potentials. (ii) TC neurones exhibit intrinsic bistable behaviour. (iii) All these properties are produced by window I_T, indicating the dramatic impact that this inactivating Ca^{2+} current has upon the electroresponsiveness of TC neurones.

Genesis of input signal amplification and bistability

Experiments and simulations indicated that input signal amplification is not formed by the activation or inactivation of Na^+, K^+ or mixed cationic currents, but is dependent upon the influence of a Ca^{2+} current. This behaviour, in fact, was abolished by a low Ca^{2+}, high Mg^{2+} medium or by addition of Ni^{2+} to the bathing solution, while an increase in $[Ca^{2+}]_o$ generated it *de novo* in neurones where it was absent in control conditions. We have shown by computer simulation that the presence of the window component of I_T may produce this behaviour when an appropriate balance between I_T and I_{Leak} exists: all experimental data are compatible with this hypothesis. In particular, the full block of input signal amplification in the absence of a full block of the LTCP, and thus of I_T (cf. Fig. 3*Ca*), indicates the critical role played in this phenomenon by the relative amplitude of I_T and I_{Leak}. In addition, the time-dependent nature of the large amplitude hyperpolarizations recorded under current clamp conditions was not reflected under voltage clamp conditions, thus supporting the hypothesis that a steady current is extant in TC neurones and that it is the voltage dependence of this steady current that affects the steady-state current–voltage relationships measured under current clamp conditions.

On the basis of these findings we propose that input signal amplification and bistability are formed according to the following scheme (Fig. 9). (i) In a voltage range centred around −60 mV, the membrane potential of TC neurones is controlled by the balance of the transmembrane currents window I_T and I_{Leak}, where I_T mediates inward and I_{Leak} outward current. This balance creates one unstable (UP) and two stable points (USP and LSP) (Fig. 9). (ii) Negative voltage responses originating from USP are amplified when I_{Leak} becomes the dominant current in the voltage range between UP and LSP, thus producing membrane hyperpolarization. Large amplitude voltage responses, therefore, occur as a consequence of the interaction between the linear voltage dependence of I_{Leak} and the exponential voltage dependence of window I_T. (iii) Membrane hyperpolarization brings about the activation of I_h that mediates membrane depolarization, and the consequential re-activation of I_T, leading to the generation of a LTCP, crowned by the burst firing of action potentials, and the recrudescence of the window component. The membrane potential will then

settle at the value corresponding to USP. (iv) Following the blockade of I_h, bistable behaviour will occur, since the membrane potential will not be repolarized by I_h and will thus remain at the most negative equilibrium voltage (corresponding to LSP). Transition to the more positive equilibrium voltage may only occur if a depolarization of magnitude sufficient to restore the balance between window I_T and I_{Leak}, i.e. capable of moving the membrane potential to values more positive than that corresponding to UP, is generated.

The reasons for the differential expression of input signal amplification and bistability between neurones are of importance. For a given I_T and I_{Leak}, input signal amplification and bistability will occur at some value of the injected DC if, and only if, the maximal slope of window I_T is greater than g_{Leak}, i.e. $(dI_{T,window}/dV)_{max} > g_{Leak}$ (Fig. 9). Since this derivative is proportional to $g_{T,max}$, it follows that $g_{T,max}/g_{Leak}$ will then exceed the constant: $1/\{d[m_\infty^3 h_\infty(V - V_{Ca})]/dV\}_{max}$ (as indicated by the simulation results). Therefore, neurones that exhibit input signal amplification may have either an unusually large I_T, or a relatively small I_{Leak} (Fig. 9). Attempts to voltage clamp I_T to ascertain its maximal amplitude and steady-state activation and inactivation values, however, were unsuccessful since it was difficult to control this current adequately when recording under conditions in which input signal amplification was manifest. We, therefore, cannot discount the possibility that TC neurones exhibiting input signal amplification have a greater than normal amplitude of I_T, or that the steady-state activation and inactivation curves of this current are shifted to produce a voltage overlap greater than normal. Experimental evidence, however, indicated that input signal amplification may be unmasked by modulation of I_{Leak}, as the application of Ba^{2+} (this study) or a metabotropic glutamate receptor agonist (J. P. Turner & T. E. Salt, personal communication), agents that reduce g_{Leak} in TC neurones (Jahnsen & Llinás, 1984*b*; McCormick & Pape, 1990; McCormick & von Krosigk, 1992), lead to the formation of input signal amplification in neurones that did not show this behaviour under control conditions. We therefore suggest that neurones that exhibit input signal amplification properties are not a specialized group of TC neurones, but are neurones that have been minimally damaged by penetration with sharp microelectrodes, and so have low values of somal shunt (Holmes & Rall, 1992; Spruston & Johnston, 1992) or distributed injury conductances (Staley, Otis & Mody, 1992), indicating that this is the true electrophysiological state of TC neurones maintained in tissue slices and perhaps *in vivo*. Since I_T is not only expressed by TC neurones but it is distributed widely across the central nervous system (Llinás, 1988; Deisz, Fortin & Zieglgansberger, 1991; Soong, Stea, Hodson, Dudel, Vincent & Snutch, 1993; Huguenard, 1996), we predict that input signal amplification will be manifest in other types of central neurones that possess I_T, and suggest that it is the product of sharp microelectrode-induced cellular damage that has prevented its observation. Furthermore, as I_T has been shown to be located in the distal dendrites of some central neurones (Magee & Johnston, 1995), the expression of input signal amplification may be facilitated in these small calibre structures because of their relatively low input conductance.

Physiological implications

The functional expression of input signal amplification *in vivo* may, therefore, be determined by a modulation of g_{Leak}. The activation of a number of different neurotransmitter receptors on TC neurones has been shown to decrease g_{Leak} (McCormick, 1992). Therefore, the expression of input signal amplification *in vivo*, may be modulated by the activity of brainstem and cortical neurones. Furthermore, since the input conductance of neurones has been demonstrated by modelling studies to be influenced by the level of background synaptic activity (Bernander, Douglas, Martin & Koch, 1991; Rall, Burke, Holmes, Jack, Redman & Segev, 1992), it is conceivable that the electroresponsiveness of TC neurones may be determined by activity within afferent pathways, with input signal amplification being replaced by more linear behaviour as activity is increased. This suggestion indicates that input signal amplification may be a process by which neurones show increased sensitivity to small amplitude isolated synaptic inputs (i.e. novel stimuli) via the generation of action potential burst firing, a mechanism that may act to initiate network operations (Steriade *et al.* 1993).

TC neurones have been observed to fire bursts of action potentials during different states of arousal (Steriade, Apostol & Oakson, 1971; McCormick, 1992; Steriade *et al.* 1993; Guido & Weyland, 1995). Such firing has been suggested to result from the generation of LTCPs superimposed upon EPSPs or following the termination of IPSPs (Jahnsen & Llinás, 1984*a*; Crunelli *et al.* 1987*a*; Crunelli & Leresche, 1991; Bal, von Krosigk & McCormick, 1995). Because of the voltage dependence of the activation and inactivation properties of I_T, it has been suggested that burst responses evoked by EPSPs or IPSPs may only occur when the membrane potential is set to values more negative or positive than around −65 mV, respectively. This interpretation has strongly influenced ideas concerning the setting of the membrane potential of different neurones within the thalamocortical network during different stages of arousal (see Steriade *et al.* 1993) and in neurological disorders (Avoli, Gloor & Kostopoulos, 1990). In the present study, we have shown that burst responses may be evoked by different forms of input: so, for example, from holding potentials set more positive than −65 mV, large amplitude hyperpolarizing voltage responses terminated by the burst firing of action potentials, were triggered by small (< 5 mV), physiologically relevant, postsynaptic potentials irrespective of their sign (excitatory or inhibitory) or duration. Therefore, from the same holding potential the formation of burst firing in TC neurones is not ruled by the form of driving postsynaptic potentials, a result that should be borne in mind when interpreting the synaptic mechanisms

that lead to the formation of burst responses in alert animals (Guido & Weyland, 1995) and in pathological disorders such as absence epilepsy (Avoli *et al.* 1990).

The temporal structure of input signal amplification was influenced by g_h, so that as g_h was decreased the duration of the voltage responses initially formed by the influence of window I_T were prolonged and as g_h approached zero bistable behaviour emerged. Previous observations have indicated that bistable behaviour may be formed by the activation of a persistent Na^+ current (Llinás & Sugimori, 1980; Jahnsen & Llinás, 1984*a*,*b*) or high-threshold Ca^{2+} currents (Hounsgaard & Kiehn, 1989). The form of bistable behaviour described in the present study is, to our knowledge, the first to be apparent at membrane potentials subthreshold for action potential generation. In TC neurones, neuromodulation of the voltage dependence of I_h activation has been implicated in the process by which the membrane potential of TC neurones is dependent upon the state of arousal (McCormick, 1992; Steriade *et al.* 1993). Various neurotransmitters have been demonstrated to shift the activation curve of I_h in the positive or negative direction (McCormick, 1992). As I_h controls the duration of voltage responses triggered by the removal of window I_T, our results indicate that the input–output relationship of TC neurones may be state dependent, with relatively longer responses being favoured when the activation curve of I_h is shifted in the negative direction. Conceivably, small amplitude, single or summated postsynaptic potentials could switch the membrane potential of neurones from one equilibrium potential to another. This process may be apparent in central neurones that express I_T but not I_h, and perhaps in TC neurones following a large negative shift in the activation range of I_h; the fast switching of the membrane potential either toward or away from the threshold for the generation of action potentials will have a profound influence upon neuronal excitability.

In conclusion, the unique electrophysiological properties of TC neurones observed in this study demonstrates a specific type of non-linear behaviour in central neurones. The involvement of window I_T in the formation of such activity indicates that the window component of inactivating membrane currents cannot be ignored in the interpretation of neuronal behaviour.

Antal, K., Emri, Zs., Tóth, T. I. & Crunelli, V. (1996). Model of a thalamocortical neurone with dendritic voltage-gated ion channels. *NeuroReport* **7**, 2655–2658.

Avoli, M., Gloor, P. & Kostopoulos, G. (1990). Focal and generalized epileptiform activity in the cortex: in search of differences in synaptic mechanisms, ionic movements, and long-lasting changes in neuronal excitability. In *Generalized Epilepsy Neurobiological Approaches*, ed. Avoli, M., Gloor, P., Kostopoulos, G. & Naquet, R., pp. 213–231. Birkhauser, Boston, MA, USA.

Bal, T., von Krosigk, M. & McCormick, D. A. (1995). Synaptic and membrane mechanisms underlying synchronized oscillations in the ferret lateral geniculate nucleus *in vitro*. *Journal of Physiology* **483**, 641–663.

Barlow, R. B. (1990). Cumulative frequency curves in population analysis. *Trends in Pharmacological Sciences* **11**, 404–406.

Bernander, O., Douglas, R. J., Martin, K. A. C. & Koch, C. (1991). Synaptic background activity influences spatiotemporal integration in single pyramidal cells. *Proceedings of the National Academy of Sciences of the USA* **88**, 11569–11573.

Coulter, D. A., Huguenard, J. R. & Prince, D. A. (1989). Calcium currents in rat thalamocortical relay neurones: kinetic properties of the transient low-threshold current. *Journal of Physiology* **414**, 587–604.

Crunelli, V., Kelly, J. S., Leresche, N. & Pirchio, M. (1987*a*). On the excitatory post-synaptic potential evoked by stimulation of the optic tract in the rat lateral geniculate nucleus. *Journal of Physiology* **384**, 603–618.

Crunelli, V. & Leresche, N. (1991). A role for $GABA_B$ receptors in excitation and inhibition of thalamocortical cells. *Trends in Neurosciences* **14**, 16–21.

Crunelli, V., Leresche, N. & Parnavelas, J. G. (1987*b*). Membrane properties of morphologically identified X and Y cells in the lateral geniculate nucleus of the cat *in vitro*. *Journal of Physiology* **390**, 243–256.

Crunelli, V., Lightowler, S. & Pollard, C. E. (1989). A T-type Ca^{2+} current underlies low-threshold Ca^{2+} potentials in cells of the cat and rat lateral geniculate nucleus. *Journal of Physiology* **413**, 543–561.

Crunelli, V., Williams, S. R., Turner, J. P., Hughes, S. W. & Tóth, T. I. (1997). Physiological expression of the 'window' component of I_T in rat and cat thalamocortical neurones *in vitro*. *Journal of Physiology* **501.P**, 25*P*.

Deisz, R. A., Fortin, G. & Zieglgansberger, W. (1991). Voltage dependence of excitatory postsynaptic potentials of rat neocortical neurons. *Journal of Neurophysiology* **65**, 371–382.

Deschênes, M., Paradis, M., Roy, J. P. & Steriade, M. (1984). Electrophysiology of neurons of lateral thalamic nuclei in cat: resting properties and burst discharges. *Journal of Neurophysiology* **51**, 1196–1219.

Guido, W. & Weyland, T. (1995). Burst responses in thalamic relay cells in the awake behaving cat. *Journal of Neurophysiology* **74**, 1782–1786.

Guyon, A. & Leresche, N. (1996). Modulation by different $GABA_B$ receptor types of voltage activated calcium currents in rat thalamocortical neurones. *Journal of Physiology* **485**, 29–42.

Harris, N. C. & Constanti, A. (1995). Mechanisms of block by ZD 7288 of the hyperpolarization-activated inward rectifying current in guinea-pig substantia nigra neurons *in vitro*. *Journal of Neurophysiology* **74**, 2366–2378.

Hernandez-Cruz, A. & Pape, H.-C. (1989). Identification of two calcium currents in acutely dissociated neurons from the rat lateral geniculate nucleus. *Journal of Neurophysiology* **61**, 1270–1283.

Holmes, W. R. & Rall, W. (1992). Electrotonic length estimates in neurons with dendritic tapering or somatic shunt. *Journal of Neurophysiology* **68**, 1421–1437.

Hounsgaard, J. & Kiehn, O. (1989). Serotonin-induced bistability of turtle motoneurones caused by nifedipine-sensitive calcium plateau potential. *Journal of Physiology* **414**, 265–282.

Huguenard, J. R. (1996). Low-threshold calcium currents in central nervous system neurons. *Annual Review of Physiology* **58**, 329–348.

Jahnsen, H. & Llinás, R. (1984*a*). Electrophysiological properties of guinea-pig thalamic neurones: an *in vitro* study. *Journal of Physiology* **349**, 205–226.

JAHNSEN, H. & LLINÁS, R. (1984*b*). Ionic basis for the electroresponsivness and oscillatory properties of guinea-pig thalamic neurones *in vitro*. *Journal of Physiology* **349**, 227–247.

LERESCHE, N., LIGHTOWLER, S., SOLTESZ, I., JASSIK-GERSCHENFELD, D. & CRUNELLI, V. (1991). Low-frequency oscillatory activities intrinsic to rat and cat thalamocortical cells. *Journal of Physiology* **441**, 155–174.

LLINÁS, R. & SUGIMORI, M. (1980). Electrophysiological properties of *in vitro* Purkinje cell somata in mammalian cerebellar slices. *Journal of Physiology* **305**, 171–195.

LLINÁS, R. R. (1988). The intrinsic electrophysiological properties of mammalian neurons: insights into central nervous system function. *Science* **242**, 1654–1664.

MCCORMICK, D. A. (1991). Functional properties of a slowly inactivating potassium current in guinea pig dorsal lateral geniculate relay neurons. *Journal of Neurophysiology* **66**, 1176–1189.

MCCORMICK, D. A. (1992). Neurotransmitter actions in the thalamus and cerebral cortex and their role in modulation of thalamocortical activity. *Progress in Neurobiology* **39**, 337–388.

MCCORMICK, D. A. & HUGUENARD, J. R. (1992). A model of the electrophysiological properties of thalamocortical neurons. *Journal of Neurophysiology* **68**, 1384–1400.

MCCORMICK, D. A. & PAPE, H.-C. (1990). Properties of a hyperpolarization-activated cation current and its role in rhythmic oscillations in thalamic relay neurones. *Journal of Physiology* **431**, 291–318.

MCCORMICK, D. A. & VON KROSIGK, M. (1992). Corticothalamic activation modulates thalamic firing through 'metabotropic' receptors. *Proceedings of the National Academy of Sciences of the USA* **89**, 2774–2778.

MAGEE, J. C. & JOHNSTON, D. (1995). Synaptic activation of voltage-gated channels in the dendrites of hippocampal pyramidal neurons. *Science* **268**, 301–304.

RALL, W., BURKE, R. E., HOLMES, W. R., JACK, J. J. B., REDMAN, S. & SEGEV, I. (1992). Matching dendritic neuron models to experimental data. *Physiological Reviews* **72**, 159–186.

SOONG, T. W., STEA, A., HODSON, C. D., DUDEL, S. J., VINCENT, S. R. & SNUTCH, T. P. (1993). Structure and functional expression of a member of the low voltage-activated calcium channel family. *Science* **260**, 1133–1136.

SPRUSTON, N. & JOHNSTON D. (1992). Perforated patch-clamp analysis of the passive properties of three classes of hippocampal neurons. *Journal of Neurophysiology* **67**, 508–529.

STALEY, K. J., OTIS, T. S. & MODY, I. (1992). Membrane properties of dentate gyrus granule cells: comparison of sharp and whole cell recordings. *Journal of Neurophysiology* **67**, 1346–1358.

STERIADE, M., APOSTOL, V. & OAKSON, G. (1971). Control of unitary activities in cerebellothalamic pathway during wakefulness and synchronized sleep. *Journal of Neurophysiology* **34**, 389–413.

STERIADE, M., CURRÓ DOSSI, R. & NUÑEZ, A. (1991). Network modulation of a slow intrinsic oscillation of cat thalamocortical neurons implicated in sleep delta waves: cortically induced synchronization and brainstem cholinergic suppression. *Journal of Neuroscience* **11**, 3200–3217.

STERIADE, M., MCCORMICK, D. A. & SEJNOWSKI, T. J. (1993). Thalamocortical oscillations in the sleeping and aroused brain. *Science* **262**, 679–685.

TÓTH, T. & CRUNELLI, V. (1992). Computer simulation of the pacemaker oscillation in thalamocortical cells. *NeuroReport* **3**, 62–66.

TÓTH, T. I. & CRUNELLI, V. (1993). Bifurcation analysis of a biophysical model of a thalamocortical cell. *Society for Neuroscience Abstracts* **19**, 219.8.

TÓTH, T. I., WILLIAMS, S. R., TURNER, J. P. & CRUNELLI V. (1995). Voltage and temporal amplification in thalamocortical (TC) neurones – Simulation studies. *Society for Neuroscience Abstracts* **21**, 47.10.

TRAUB, R. D., WONG, R. K. S., MILES, R. & MICHELSON, H. (1991). A model of a CA3 hippocampal pyramidal neuron incorporating voltage-clamp data on intrinsic conductances. *Journal of Neurophysiology* **66**, 635–650.

TURNER, J. P., ANDERSON, C. M., WILLIAMS, S. R. & CRUNELLI, V. (1997). Morphology and membrane properties of neurones in the cat ventrobasal thalamus *in vitro*. *Journal of Physiology* **505**, 707–726.

TURNER, J. P., LERESCHE, N., GUYON, A., SOLTESZ, I. & CRUNELLI, V. (1994). Sensory input and burst firing output of rat and cat thalamocortical cells: the role of NMDA and non-NMDA receptors. *Journal of Physiology* **480**, 281–295.

UCHIMURA, N., CHERUBINI, E. & NORTH, R. A. (1989). Inward rectification in rat nucleus accumbens neurons. *Journal of Neurophysiology* **62**, 1280–1286.

WILLIAMS, S. R., TURNER, J. P., ANDERSON, C. M. & CRUNELLI, V. (1996). Electrophysiological and morphological properties of interneurones in the rat lateral geniculate nucleus *in vitro*. *Journal of Physiology* **490**, 129–147.

WILLIAMS, S. R., TURNER, J. P., HUGHES, S. W. & CRUNELLI, V. (1997). On the nature of anomalous rectification in thalamocortical neurones of the ventro-basal thalamus *in vitro*. *Journal of Physiology* **505**, 727–747.

WILLIAMS, S. R., TURNER, J. P., TÓTH, T. I. & CRUNELLI, V. (1995). Voltage and temporal amplification in thalamocortical (TC) neurones – Experimental studies. *Society for Neuroscience Abstracts* **21**, 47.9.

Acknowledgements

We would like to thank Caroline M. Anderson, Tim M. Gould, Bob M. Jones and Susan H. Price for their assistance. We thank Dr H. Rhein Parri and Professor D. I. Wallis for their comments on a previous version of the manuscript. The support of The Wellcome Trust (grant no. 37089) is gratefully acknowledged. S.R.W. and S.W.H. were Wellcome Prize Students.

Authors' present addresses

S. R. Williams: Reed Neurological Research Center, UCLA School of Medicine, Los Angeles CA 90024, USA.

J. P. Turner: Department of Visual Science, Institute of Opthalmology, London EC1V 9EL, UK.

Author's email address

V. Cruneli: crunelli@cardiff.ac.uk

Received 28 April 1997; accepted 12 August 1997.